Research Article | Vol. 29, No. 20 / 27 Sep 2021 / Optics Express 31499
Optics EXPRESS

Real-time stimulated Raman spectroscopy with a non-collinear optical parametric oscillator

LUISE BEICHERT,[1,2,*] YULIYA BINHAMMER,[1,2] JOSÉ R. C. ANDRADE,[3] ROBIN MEVERT,[1,2] ANN-KATHRIN KNIGGENDORF,[4] BERNHARD ROTH,[2,4] AND UWE MORGNER[1,2]

[1]*Institute of Quantum Optics, Leibniz Universität Hannover, Welfengarten 1, 30167 Hannover, Germany*
[2]*Cluster of Excellence PhoenixD (Photonics, Optics, and Engineering Innovation Across Disciplines), Hannover, Germany*
[3]*Max Born Institute for Nonlinear Optics and Short Pulse Spectroscopy, Max-Born-Straße 2a, 12489 Berlin, Germany*
[4]*Hannover Centre for Optical Technologies, Leibniz Universität Hannover, Nienburger Str. 17, 30167 Hannover, Germany*
[*]*beichert@iqo.uni-hannover.de*

Abstract: Ultrafast detection of microplastic particles is becoming a vital problem, as these particles are found in water sources worldwide. Ideally, a live analysis in flow is desirable to directly monitor the water quality for contaminations. Therefore, coherent Raman spectroscopy techniques require fast and broadband tunable lasers to address all relevant spectral regions of the investigated samples. In our work, we combine a high power non-collinear optical parametric oscillator with a real-time stimulated Raman scattering spectroscopy setup. The light source is continously tunable from 700 nm to 1030 nm in less than 10 ms, delivering an average output power of more than 500 mW with sub-ps pulses. We show the immediate observation of mixing processes and the detection of microplastic particles in water solution with a spectral window of more than 2000 cm^{-1}.

1. Introduction

Stimulated Raman Scattering (SRS) gives label-free access to the vibrational information of molecules. Since its discovery in 1962 [1] this technique developed rapidly and is in interdisciplinary use, not only in biomedical applications, but also in chemistry and material sciences [2]. Spectroscopy through SRS is an important tool for studying for example microplastic particles (MP) [3], which are widely spread in our global environment. The current research is concerned with the biological and ecological impact of the MP, as well as with their detection and identification. However, with the current technology the latter is still a challenge in liquid samples.

A detailed description of SRS can be found in seminal textbooks [4,5] and in numerous review-papers [6,7]. In brief, a stimulated Raman setup consists of two laser beams with different wavelengths: the pump at frequency ω_p and the Stokes wave ω_s, both focused into a sample. If the difference frequency matches a molecular vibration of the sample $\Omega_{vib} = \omega_p - \omega_s$, a part of the pump beam is transferred to the Stokes beam due to the coherent excitation of the molecular vibration. This can be measured as stimulated Raman gain (SRG) ΔI_s or stimulated Raman loss (SRL) ΔI_p. As the intensity change is very small ($\Delta I/I \approx 10^{-6}$), SRS usually involves high-frequency amplitude modulation in combination with a lock-in amplifier detection scheme.

To analyse the Raman response for various wavenumbers, either the pump or the Stokes beam needs to be changed in frequency. Optical Parametric Oscillators (OPOs) are suitable light sources, as they provide the required tunablity over a wide range. Moreover, with the pump source of the OPO, a synchronized second beam with a second color is already at hand. Common

#436318 https://doi.org/10.1364/OE.436318
Journal © 2021 Received 7 Jul 2021; revised 17 Aug 2021; accepted 17 Aug 2021; published 16 Sep 2021

Optics EXPRESS

schemes to shift the narrowband OPO output are pump wavelength, temperature, or crystal angle tuning [8]. Unfortunately, these methods are comparably slow and retard the spectroscopy process. Kong et al. [9] use an intra-cavity electro-optical Lyot filter that switches the wavelength every 5 ms; but the tuning range spans only 7.5 nm. Likewise, Brinkmann et al. [10] reach a tuning speed of 5 ms per wavelength step with a fiber-based OPO. There, rapid tunability between 780 nm to 980 nm is achieved by an electronically tunable wavelength filter and a special chirped fiber Bragg grating as output coupler.

Instead of directly tuning the lightsource, other schemes for fast hyperspectral SRS have been established. A good overview can be found in [11]. One common technique is the spectral focusing method. Here, two broadband laser outputs with a strong chirp are temporally delayed against each other. The frequency difference can be tuned via a motorized stage [12] or with a rapid acousto-optic delay line. Alshaykh et al. [13] succeeded with this procedure in a scan rate of 30 kHz for a 200 cm^{-1} cm^{-1} spectral window.

Another technique is multiplex SRS. By using one narrow and one broadband detection beam, one can observe many spectral lines simultaneously [14] with a multichannel photodiode array. Zhang et al. [15] achieved with a 32-channel array acquisition times of 5 µs per SRS spectrum over a spectral range of 200 cm^{-1}. Also a combination of spectral focusing and multiplex SRS have been shown [16].

In this paper, we report on fast SRS directly from a widely tunable non-collinear optical parametric oscillator (NOPO). NOPOs were demonstrated in the near-IR [17] and in the visible [18] spectral regime. They allow for a ultra broadband tuning range by solely changing the cavity length. More than 100 nm/ms tuning speeds are possible. Through wavelength switching even 1000 nm/ms are possible [19]. In comparison to the multiplex SRS, our approach includes a very simple setup with only one photodiode and a lock-in amplifier. Neither spectral diffraction nor elaborate optics such as dispersive elements, white light generation or adaptive pulse shapers are required. Nevertheless, we can detect broadband SRS spectra, spanning a spectral window over 2000 cm^{-1} in less than 8 ms. As an example, we observe mixing processes in liquids, as well as quickly moving polyamide microplastic particles in a water solution within video-rates. This, in the future, might allow for reliable continuous monitoring of MP in flowing water sources.

2. Experimental setup

2.1. NOPO

The NOPO setup follows the description in [17]. A sketch is shown in Fig. 1 on the left. The centerpiece is a 2 mm β-Barium-Borate crystal (BBO) with the phase matching angle $\Theta = 26.4°$, placed in Brewster's angle. It offers broadband phase matching from 650 nm to 1030 nm under a non-collinear angle of 2.4°. The pump radiation is produced by a home-built Kerr-lens mode-locked Yb:YAG thin disk (KLM TD) laser [20]. The pump laser delivers 25 W average output power at 1030 nm and a repetition rate of 34 MHz. The FWHM pulse duration is measured around 300 fs. In order to pump the NOPO, 9.5 W of the IR-light are frequency doubled in a 2 mm Lithium Triborate crystal (LBO) in single-pass configuration to more than 7.5 W green light at 515 nm. This corresponds to an efficiency of 70 %. The pulse energy behind the crystal amounts 0.2 µJ. Subsequently, the radiation is focused into the gain crystal.

The cavity consists of two curved mirrors with a radius of curvature of −100 mm and seven plane double chirped mirrors (DCMs), which support a spectral range from 600 nm to 1200 nm, plus an output coupler with a transmission of 12 % in standing wave geometry. The cavity length of 4.4 m is adapted to the repetition rate of the KLM TD pump laser. Two 12 mm fused silica plates introduce over four passes an internal dispersion of approximately 3500 fs^2 respectively at a central wavelength of 800 nm. One cavity mirror is placed on a piezoelectric actuator (Thorlabs, PK2FVF1). The change in cavity length determines which spectral portion of the chirped signal experiences gain from the narrowband pump pulse and gets amplified. Just by moving the mirror,

Optics EXPRESS

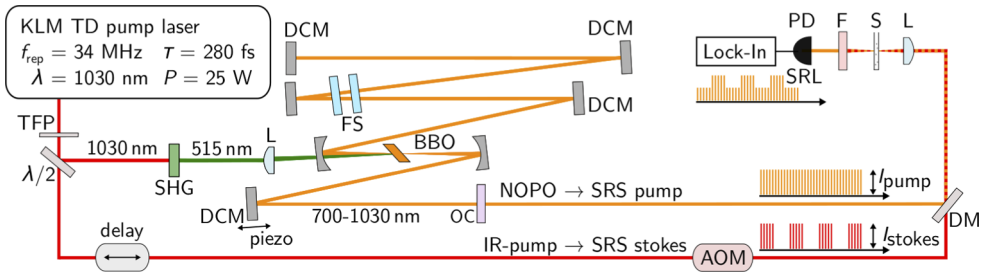

Fig. 1. Left: NOPO setup: KLM TD: Kerr-lens mode-locked thin-disk laser, TFP: thin-film polarizer, SHG: 2.5 mm LBO crystal for SHG, L: lens, BBO: gain crystal, DCM: double-chirped mirror, FS: fused silica plate, OC: output coupler. Right: SRS setup: AOM: acousto-optic modulator, DM: dichroic mirror, S: sample, PD: photo diode, SRL: stimulated Raman Loss.

the NOPO is tunable from 700 nm to the degeneracy point at 1030 nm with a spectral bandwidth between 2.7 THz for the shortest wavelength and up to 5 THz when close to the degeneracy. The output power reaches easily more than 500 mW. At a central wavelength of 800 nm it can be scaled even to 1 W by increasing the pump power. Since this operating point is close to the damage threshold of the nonlinear crystals, the NOPO runs routinely with the mentioned parameters. The tuning behavior is shown in Fig. 2.

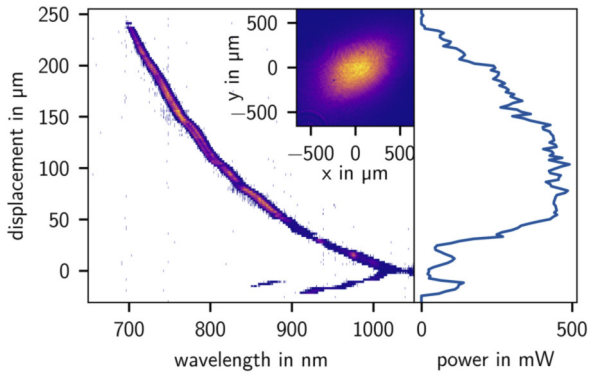

Fig. 2. The tuning behavior of the NOPO depends on the displacement of the cavity length. The output power (right) outreaches 500 mW. The output spectrum (left) spans from 700 nm to 1030 nm with the spectral bandwidth $\Delta\lambda \approx 4.5nm$ for shorter wavelength and up to 10 nm close to the degeneracy point. The beam profile in the inset shows a slight ellipticity.

We operate the NOPO in the Poynting vector walk-off compensation geometry. This typically results in a better beam profile but affects the tunability due to a parasitic second harmonic generation around 900 nm [21]. This leads to strong cavity fluctuations and a drop in output power at this wavelength, which prohibits SRS measurements around 1400 cm^{-1}.

2.2. SRS

The compact spectroscopic setup (Fig. 1, right) is kept basic. The tunable NOPO output acts as pump source for the SRS process. Some remaining light form the KLM TD laser is used as Stokes beam, so no additional synchronization is needed.

By using a delay line and a dichroic mirror both beams are temporally and spatially overlapped. An acousto-optic modulator (IntraAction Corp., AOM-405A1) alters the amplitude of the Stokes

Optics EXPRESS

beam with a frequency of 1 MHz and a modulation depth of 75 %. A lens (f = 50 mm) focuses the beams into the sample to beam waists around 25 µm. As the focussing is low compared to typical SRS microscopy setups (e.g. [22]) both beams need an average power around 260 mW reaching intensities of approximately 25 kW/cm^2 in the probe. A shortpass filter (Thorlabs, FESH950) removes the Stokes beam, so that only the pump light is detected on a large-area photodiode (Thorlabs, FDS100). A neutral density filter with an optical density of OD=1.0 protects the diode against saturation. As sufficiently high intensities in the samples are needed for the SRS process, it is impossible to work with lower input powers. Furthermore, a reduction of the pump power from the KLM TD laser would reduce the tuning range of the NOPO. By a lock-in amplifier (Stanford Research Systems, SR865A) the SRL is measured with integration time constants down to 1 µs.

3. Experiments and results

3.1. Measurement principle

We explain the measurement procedure using a stationary water sample. For tuning, a triangle voltage is applied to the piezo actuator. A slow measurement assigns the voltage to the corresponding wavelength. The voltage on the electronic translation stage is increased step-wise. For each monitoring point the NOPO average output power is measured with a thermal power sensor (Thorlabs, S425C-L) as well as its output spectrum (OceanOptics, USB4000, 530 nm to 1200 nm). Power and wavelength calibrations are shown in Fig. 3(a)-(c).

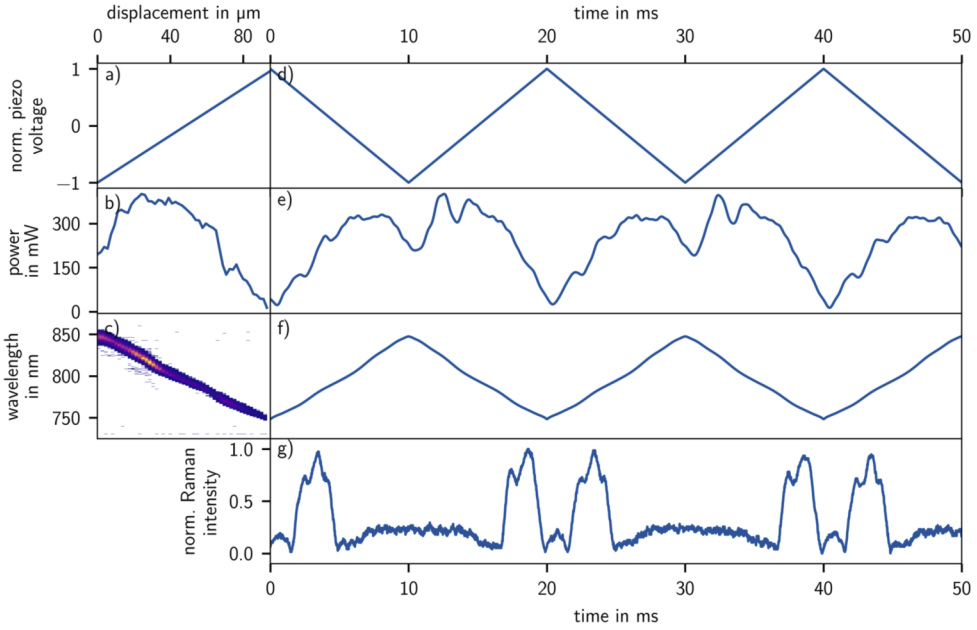

Fig. 3. a) Voltage on the piezoelectric actuator, b) NOPO average output power and c) spectra over the displacement of the cavity length during a slow calibration measurement. Accordingly in the course of the fast measurement d) voltage, e) power and f) central output wavelength are determined over time. Graph f) shows the corresponding wavelengths from the slow measurement in c). g) Raman signal over time detected on the lock-in amplifier from a pure water sample.

For the real-time measurements, we apply triangle voltages with frequencies between 50 Hz and 65 Hz to the piezo actuator. As we can measure Raman spectra in the forward and backward

Optics EXPRESS

direction of the mirror movement this corresponds to scanning times between 7.7 ms and 10 ms. We monitor the piezo voltage displayed in Fig. 3(d) and the Raman intensity from the lock-in amplifier in Fig. 3(g). In Fig. 3 on the right side we show an example with a pure water sample in a 2 mm sized cuvette. The NOPO wavelength is tuned between 750 nm and 850 nm in 10 ms. As the spectrometer can not follow the fast wavelength changes, Fig. 3(f) shows the determined central wavelength according to the slow measurement in c). The output power is tracked in real-time with a photodiode shown in Fig. 3(e). The NOPO output power curve in Fig. 3(e) and the Raman signal in g) show a small hysteresis from the mirror motion, so that there are slight differences during forward and backward motion. Furthermore, near the edges of the wavelength range, when the mirror changes its direction, the assignment between voltage and wavenumber is distorted. Nevertheless, in the center part, the mirror performs a linear motion and we can obtain reliable Raman spectra from 2000 cm^{-1} to 3600 cm^{-1}. The measured SRS spectra are in good agreement with the Raman spectra from the references, as can be seen in the following measurements.

3.2. Mixing processes in liquids and concentration determination

Next, we study mixing processes in liquids. The samples are illuminated in a fused silica glass cuvette with a geometrical path length of 1 cm. In Fig. 4(a), Raman spectra for different concentrations of a water-isopropyl mixture are shown. Each spectrum is averaged from 17 individual ones, taken altogether in 260 ms. Due to the hysteresis, only every second spectrum was considered. The water shows a strong characteristic Raman line from the predominant OH-stretching mode around 3400 cm^{-1}, while isopropyl has only a very weak Raman response in this region. Therefore it features a strong line at 2900 cm^{-1} due two the CH_3-stretching modes [23]. The SRS signal is linear to the number of excited molecules and thus to the concentration in mixtures. In Fig. 4(b) the Raman intensity ratio I_{water}/I_{iso} of the two signals is plotted over the mixing ratio V_{water}/V_{iso}. The individual intensities are extracted from the above measurements by taking the maximum peak values in the specific wavenumber range for isopropyl and water. The line of best fit coincides very well with the data points with the coefficient of determination $R^2 = 0.99988$. Thereby the two extreme points indicating only water and only isopropyl were not taken into account.

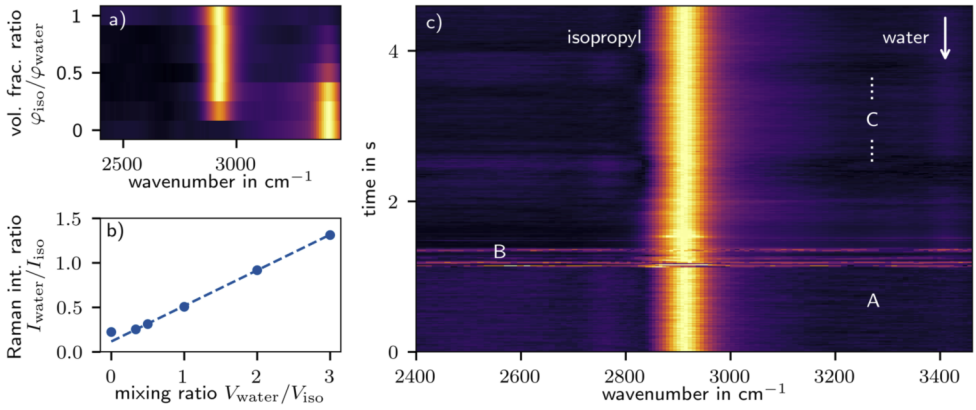

Fig. 4. a) Raman spectra of water-isopropyl mixtures with different concentrations. On the vertical axis is the volume fraction ratio. b) Linear progression of the Raman intensity ratio as a function of the mixing ratio. c) Time series of Raman spectra detected within a rate of 130 Hz or one spectrum in 7.7 ms. After 1.2 s (B) one drop water is added to the pure isopropyl sample. The mixing process forms strong streaks and takes 150 ms. Afterwards, the mixing concentration is determined to V_{water}/V_{iso} = 46 µl/400 µl.

Optics EXPRESS

The right graph Fig. 4(c) shows a real time measurement from a pure 40 µl isopropyl sample.(A). The SRS setup is the same as described in the previous part. The Raman signal is continuously monitored on an oscilloscope. It stays unchanged till after 1.2 s one water droplet is added by hand with a pipette to the unclosed cuvette. As water-alcohol-mixtures form streaks, the Raman signal is strongly disturbed during the mixing process (B). After 150 ms it calms down and a small water signal at 3410 cm^{-1} is observable. Beyond that point, there are still slower oscillations in the mixture with a period of 1.3 s (C), recognizable by a drop of the water peak strength at 2.6 s and 3.9 s. Finally, the volume ratio and thus the droplet volume can be determined from the derived Raman intensity ratio after the mixing process with the help of the line of best fit in Fig. 4(b). It is calculated to be 46 µl. This agrees very well with the typical droplet size from the used pipette. A filling level of 1.5 µl produce 36 droplets, resulting in an average droplet volume of 42 µl.

3.3. Microplastic particles in water

Furthermore, with this setup we show the detection of polyamide (PA) microplastic particles (MP) in a water volume in real-time. PA consist of long-chain hydrocarbon compounds. Related to the isopropyl in the previous section it shows strong characteristic lines around 2900 cm^{-1} based on the CH_2-stretching [24]. The size of the particles (Carl Roth, PA for column chromatography, 9620) varies between 50 µm and 160 µm. For comparison, the Gaussian beam waist of the pump and Stokes beams inside the sample is around 25 µm. Since plastic particles sink in water, the fluid density needs to be adapted. Therefore, the MP float in a 19 % sodium chloride solution with a density of 1.13 g/cm^3. The solved ions do not show any Raman contribution. The liquid is suspended in a square cuvette made of borosilicate glass with a geometrical path length of 2 mm.

In Fig. 5(b) the time series from a 5 s-measurement is shown. The NOPO output is continuously tuned between 710 nm and 830 nm with a rate 60 Hz. This corresponds to a wavenumber range between 2300 cm^{-1} and 4300 cm^{-1}, which is detected in 8.3 ms. The strong signal at 3450 cm^{-1} originates from the water. Compared to the Raman line in the previous mixing experiments, the water signal is shifted by 40 cm^{-1}. This is caused by a slightly different position of the movable mirror and the not entirely linear movement of the piezoelectric actuator. During the measurement, four plastic particles cross the focus volume of the two detection beams. The water signal decreases and a signal at 2890 cm^{-1} occurs. Each MP is seen on 15 to 20 single spectra, on average for 130 ms.

It should be noted, that the MP signal is more than ten times smaller than the Raman signal from the water. That is why we need to work on a low sensitivity regime on the lock-in amplifier and the MP signal itself after the subtraction of the background looks noisy. However, the signal position fits accurately with the reference spectrum as can be seen in Fig. 5(a). The reference data in grey were collected using the same PA particles in a water sample via spontaneous Raman spectroscopy. The detailed setup for this measurements is described in [25].

All in all, our technique can pave the way, to a fast MP detection. In the future, the great challenge will be the design of a flow cell with a sufficient high flow rate to detect real-life MP concentrations of a few particles per litre. The ability to measure the particles and their specific Raman spectra directly in aquatic samples eliminates the need for complex filtering and reprocessing of the samples. By scaling the output power of the NOPO and by increasing the beam waists, even larger volumes can be investigated in real-time.

Optics EXPRESS

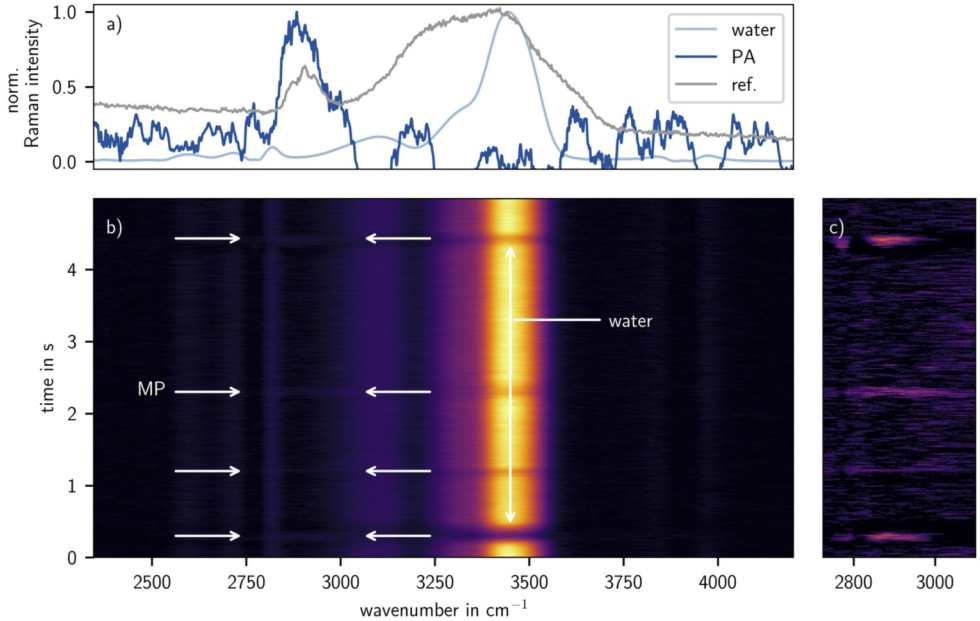

Fig. 5. a) Normalized Stimulated Raman spectra compared to reference data taken by spontaneous Raman spectroscopy (grey). bright blue: average background of the strong water signal, dark blue: single spectrum of the last polyamide particle at 4.2 s in the bottom plot after background subtraction. b) Time series of Raman spectra from the sodium chloride solution with polyamide microplastics. Arrows indicate the four particles which are measured within 5 s. The spectra are taken with a rate of 120 Hz. On average the particles stay for 130 ms in the detection area. c) Section of the time series with background subtraction to highlight the weak MP signals.

4. Conclusion

In conclusion, we introduce a very plain and fast stimulated Raman scattering setup with a non-collinear optical parametric oscillator. We can continuously detect broadband spectra in the region of the stretching modes of OH and CH/CH_2 groups from 2000 cm^{-1} to 3500 cm^{-1} in less than 8 ms. After presenting the measurement method we showed the concentration determination of an isopropyl-water mixture. Comparing the Raman intensities of the main peaks from both liquids we can observe mixing processes in real-time. Furthermore, we detected MP plastic particles directly in a water volume. The polyamide particles with up to 160 µm size, stay in average 130 ms in the detection zone. The measured SRS spectra fit very well to the Raman spectra from the literature. In addition, the sampling volume can be enlarged by scaling the NOPO output power and adapting the beam diameters. Beyond, the tuning speed can still be increased by a faster motion of the cavity mirror. Both, the necessary tuning travel distance and the bandwidth of the NOPO output spectra and thus the spectral resolution can be adjusted by the amount of internal dispersion [17]. Moreover, by changing the nonlinear crystal in the NOPO to tangential phase matching geometry, the parasitic fluctuations can be avoided at an expense of a lower-quality beam profile [21]. Then, a broader tunability range with a plateau-like output power is possible. This would permit continuous acquisition of spectra from the middle part of the fingerprint region at 800 cm^{-1} to the water peak at 3500 cm^{-1}. Such broad spectra are generally only observable in spontaneous Raman scattering. The exploitation of these prospects are subject of ongoing research. In the future, our approach might allow for the detection of various MP in environmental samples.

Optics EXPRESS

Funding. Bundesministerium für Bildung und Forschung (13N13810); Deutsche Forschungsgemeinschaft (EXC 2122, MO 850/31-1, MO 850-23/1, Project ID 390833453); Horizon 2020 Framework Programme (Marie Sklodowska-Curie Grant Agreement No. 713694.).

Disclosures. The authors declare no conflicts of interest.

Data availability. Data underlying the results presented in this paper are not publicly available at this time but maybe obtained from the authors upon reasonable request.

References

1. G. Eckhardt, R. W. Hellwarth, F. J. McClung, S. E. Schwarz, D. Weiner, and E. J. Woodbury, "Stimulated Raman Scattering From Organic Liquids," Phys. Rev. Lett. **9**(11), 455–457 (1962).
2. C. Zhang and J.-X. Cheng, "Perspective: Coherent Raman scattering microscopy, the future is bright," APL Photonics **3**(9), 090901 (2018).
3. C. Araújo, M. Nolasco, A. Ribeiro, and P. Ribeiro Claro, "Identification of microplastics using Raman spectroscopy: Latest developments and future prospects," Water Res. **142**, 426–440 (2018).
4. J.-X. Cheng and X. S. Xie, *Coherent Raman Scattering Microscopy* (CRC Press, 2012).
5. R. W. Boyd, *Nonlinear Optics* (Academic Press, Amsterdam ; Boston, 2008), 3rd ed.
6. H. Rigneault and P. Berto, "Tutorial: Coherent Raman light matter interaction processes," APL Photonics **3**(9), 091101 (2018).
7. R. C. Prince, R. R. Frontiera, and E. O. Potma, "Stimulated Raman Scattering: From Bulk to Nano," Chem. Rev. **117**(7), 5070–5094 (2017).
8. M. Ebrahimzadeh, "Mid-Infrared Ultrafast and Continuous- Wave Optical Parametric Oscillators," in *Solid-State Mid-Infrared Laser Sources*, I. T. Sorokina and K. L. Vodopyanov, eds. (Springer, Berlin, Heidelberg, 2003), Topics in Applied Physics, pp. 184–224.
9. L. Kong, M. Ji, G. R. Holtom, D. Fu, C. W. Freudiger, and X. S. Xie, "Multicolor stimulated Raman scattering microscopy with a rapidly tunable optical parametric oscillator," Opt. Lett. **38**(2), 145–147 (2013).
10. M. Brinkmann, M. Brinkmann, M. Brinkmann, A. Fast, A. Fast, T. Hellwig, T. Hellwig, I. Pence, C. L. Evans, C. Fallnich, and C. Fallnich, "Portable all-fiber dual-output widely tunable light source for coherent Raman imaging," Biomed. Opt. Express **10**(9), 4437–4449 (2019).
11. Y. Ozeki, T. Asai, J. Shou, and H. Yoshimi, "Multicolor Stimulated Raman Scattering Microscopy With Fast Wavelength-Tunable Yb Fiber Laser," IEEE J. Sel. Top. Quantum Electron. **25**(1), 1–11 (2019).
12. H. T. Beier, G. D. Noojin, and B. A. Rockwell, "Stimulated Raman scattering using a single femtosecond oscillator with flexibility for imaging and spectral applications," Opt. Express **19**(20), 18885–18892 (2011).
13. M. S. Alshaykh, C.-S. Liao, O. E. Sandoval, G. Gitzinger, N. Forget, D. E. Leaird, J.-X. Cheng, and A. M. Weiner, "High-speed stimulated hyperspectral Raman imaging using rapid acousto-optic delay lines," Opt. Lett. **42**(8), 1548–1551 (2017).
14. E. Ploetz, S. Laimgruber, S. Berner, W. Zinth, and P. Gilch, "Femtosecond stimulated Raman microscopy," Appl. Phys. B **87**(3), 389–393 (2007).
15. C. Zhang, K.-C. Huang, B. Rajwa, J. Li, S. Yang, H. Lin, C.-s. Liao, G. Eakins, S. Kuang, V. Patsekin, J. P. Robinson, and J.-X. Cheng, "Stimulated Raman scattering flow cytometry for label-free single-particle analysis," Optica **4**(1), 103–109 (2017).
16. A. D. la Cadena, C. M. Valensise, M. Marangoni, G. Cerullo, and D. Polli, "Broadband stimulated Raman scattering microscopy with wavelength-scanning detection," J. Raman Spectrosc. **51**(10), 1951–1959 (2020).
17. T. Lang, T. Binhammer, S. Rausch, G. Palmer, M. Emons, M. Schultze, A. Harth, and U. Morgner, "High power ultra-widely tuneable femtosecond pulses from a non-collinear optical parametric oscillator (NOPO)," Opt. Express **20**(2), 912–917 (2012).
18. R. Mevert, Y. Binhammer, J. Fan, T. Binhammer, C. M. Dietrich, J. R. Andrade, L. Beichert, and U. Morgner, "Femtosecond ultra-broadband non-collinear optical parametric oscillator in the visible spectral range (vis-nopo)," in *9th EPS-QEOD Europhoton Conference on Solid-State, Fibre, and Waveguide Coherent Light Sources (EUROPHOTON 2020)*, vol. Tu-P1.5 (Prague, 2020).
19. A. Pape, T. Binhammer, Y. Khanukaeva, T. Lang, J. Ahrens, O. Prochnow, and U. Morgner, "Ultrafast spectral switching of a Non-collinear Optical Parametric Oscillator (NOPO)," in *International Conference on Ultrafast Phenomena (2016)*, Paper UW4A.43, (Optical Society of America, 2016), p. UW4A.43.
20. J. R. C. Andrade, N. Modsching, A. Tajalli, C. M. Dietrich, S. Kleinert, F. Placzek, B. Kreipe, S. Schilt, V. J. Wittwer, T. Südmeyer, and U. Morgner, "Carrier-Envelope Offset Frequency Stabilization of a Thin-Disk Laser Oscillator via Depletion Modulation," IEEE Photonics J. **12**(2), 1–9 (2020).
21. T. Lang, A. Harth, J. Matyschok, T. Binhammer, M. Schultze, and U. Morgner, "Impact of temporal, spatial and cascaded effects on the pulse formation in ultra-broadband parametric amplifiers," Opt. Express **21**(1), 949–959 (2013).
22. C. W. Freudiger, W. Min, B. G. Saar, S. Lu, G. R. Holtom, C. He, J. C. Tsai, J. X. Kang, and X. S. Xie, "Label-Free Biomedical Imaging with High Sensitivity by Stimulated Raman Scattering Microscopy," Science **322**(5909), 1857–1861 (2008).

Optics EXPRESS

23. D. Lin-Vien ed., *The Handbook of Infrared and Raman Characteristic Frequencies of Organic Molecules* (Academic Press, Boston, 1991).
24. A. H. Kuptsov and G. N. Zhizhin, *Handbook of Fourier Transform Raman and Infrared Spectra of Polymers* (Elsevier, Amsterdam; New York, 1998).
25. A.-K. Kniggendorf, C. Wetzel, and B. Roth, "Microplastics Detection in Streaming Tap Water with Raman Spectroscopy," Sensors **19**(8), 1839 (2019).